

POLYCYCLIC AROMATIC HYDROCARBONS AND THE DIFFUSE INTERSTELLAR BANDS: A SURVEY

F. SALAMA

NASA-Ames Research Center, Space Science Division, Mail Stop 245-6, Moffett Field, CA 94035-1000; fsalama@mail.arc.nasa.gov

G. A. GALAZUTDINOV

Special Astrophysical Observatory, Nizhnij Arkhyz 357147, Russia; gala@sao.ru

J. KRĘŁOWSKI

Nicolaus Copernicus University, Center for Astronomy, Gagarina 11, Pl-87-100 Toruń, Poland; jacek@astri.uni.torun.pl

L. J. ALLAMANDOLA

NASA-Ames Research Center, Space Science Division, Mail Stop 245-6, Moffett Field, CA 94035-1000; lallamand@mail.arc.nasa.gov

AND

F. A. MUSAEV

Special Astrophysical Observatory, Nizhnij Arkhyz 357147, Russia; faig@sao.ru

Received 1999 February 10; accepted 1999 July 6

ABSTRACT

We discuss the proposal relating the origin of some of the diffuse interstellar bands (DIBs) to neutral and ionized polycyclic aromatic hydrocarbons (PAHs) present in interstellar clouds. Laboratory spectra of several PAHs, isolated at low temperature in inert gas matrices, are compared with the spectra of five reddened early-type stars selected from an extensive set of astronomical spectra. From this comparison, it is concluded that PAH ions are good candidates to explain some of the DIBs. Unambiguous assignments are difficult, however, because of the shift in wavelengths and the band broadening induced in the laboratory spectra by the solid matrix. This situation is illustrated by a comparison with the gas-phase spectra made available recently for two PAH ions. Definitive band assignments and, ultimately, the test of the proposal that PAH ions carry some of the DIBs must await the availability of a larger set of gas-phase measurements in the laboratory. The present assessment offers a guideline for future laboratory experiments by allowing the preselection of promising PAH molecules to be studied in jet expansions.

Subject headings: dust, extinction — ISM: abundances — line: identification — methods: laboratory

1. INTRODUCTION

Interstellar H I clouds are characterized by various absorption features that are superposed on the spectra of early-type reddened OB stars. These absorption features form several classes:

1. The continuous extinction is the selective attenuation of starlight. It is thought to be caused by interstellar dust grains (for a review, see Mathis 1990 or Kręłowski & Papaj 1993).

2. The polarization of starlight is caused by the partial alignment of the dust grains with the interstellar magnetic field (for a review, see Whittet 1996).

3. Spectral resonant lines are caused by rarefied atomic gases (most of them fall in the far-UV range; Morton 1975). The line pattern changes from object to object—e.g., Crawford (1989). In the visual wavelength range, the set of lines consists of Fraunhofer D₁ and D₂ of Na I, as well as H and K of Ca II and the weaker lines of Fe I, K I, and Ca I.

4. Absorption features of simple molecular species (CH, CH⁺, CN, C₂, NH, H₂, and CO), some of them known since the late 1930s, are detected. Their intensity-to- E_{B-V} ratios vary strongly from cloud to cloud (Crawford 1989; Kręłowski et al. 1992; Snow 1992).

5. A set of ubiquitous absorption features, the diffuse interstellar bands (DIBs), remains unidentified since its discovery by Heger in 1922. The DIB spectrum consists of more than 200 confirmed interstellar bands, including a large number of weak features. For a recent review, see Herbig (1995).

Here, we focus on the DIBs and, more specifically, on the potential link between the polycyclic aromatic hydrocarbon (PAH) ions and the carriers of the bands.

The PAH-DIB proposal was put forward, more than a decade ago, on the basis of the expected abundance of PAHs in the interstellar medium and their stability against UV photodissociation (Van der Zwet & Allamandola 1985; Léger & d'Hendecourt 1985; Crawford, Tielens, & Allamandola 1985). PAHs are now thought to be largely responsible for the discrete infrared emission bands observed at 3.3, 6.2, 7.7, 8.6, and 11.3 μm in many astronomical objects, including H II regions, planetary and reflection nebulae, and the ISM of the Milky Way and other galaxies. Recent observations from the IR space satellites *Infrared Space Observatory (ISO)* (Mattila et al. 1996) and *Infrared Telescope in Space (IRTS)* (Onaka et al. 1996) have confirmed that PAHs are ubiquitous throughout the general diffuse ISM as well. According to the astrophysical model, PAHs are expected to be present as a mixture of free, neutral and ionized, molecules following a large-sized distribution that may range from small, gas-phase, molecules (≤ 25 carbon atoms) to large graphitic platelets (Allamandola, Tielens, & Barker 1989; Puget & Léger 1989). PAHs are considered to form a link between the gas and the solid phase of interstellar dust and to be a key element for the coupling of stellar FUV photons with the interstellar gas.

Initial testing of the PAH-DIB proposal was hampered by the lack of laboratory spectra of PAHs taken under astrophysically relevant conditions. This situation has

improved, however, thanks to the laboratory studies that have been performed to measure the spectroscopic properties of neutral and ionized PAHs in astrophysically relevant media, i.e., PAHs truly isolated at low temperature (4.2 K) in neon matrices (Salama & Allamandola 1991, 1992a, 1992b, 1993; Salama, Joblin, & Allamandola 1994, 1995; Ehrenfreund et al. 1992, 1995; Léger, d'Hendecourt, & Défourneau 1995). Based on these data and on the astronomical data then available, the PAH-DIB proposal has been reassessed (Salama 1996; Salama et al. 1996) with the conclusion that PAH ions were indeed very promising candidates for the DIB carriers. Since then, both the laboratory and astronomical data sets have evolved in size considerably. An extensive set of matrix-isolated spectra of PAH ions is now available (Salama 1996; Salama, Joblin, & Allamandola 1999). Moreover, very recent follow-up experiments (Romanini et al. 1999; Bréchnignac & Pino 1999) have now opened the way for a similarly extensive study in the gas phase. Here, we compare the extensive set of laboratory spectra available for about 15 PAH ions isolated in neon matrices to an extensive set of high-resolution astronomical data. The objectives are (1) to confirm the correlations previously found between some specific PAH ions and some specific DIBs (Salama et al. 1995; Salama 1996) against higher resolution astronomical data, (2) to search for new DIBs at the positions predicted by laboratory measurements, (3) to present a set of potential PAH candidates for studies in the gas phase, and (4) to further assess and test the validity of the PAH-DIB proposal.

In § 2 we briefly review the current state of knowledge regarding the DIBs. This is followed, in §§ 3 and 4, by a description of the astronomical and laboratory data sets, respectively. In § 5, we discuss the results of this assessment.

2. DIFFUSE INTERSTELLAR BANDS

The DIBs are absorption features superposed on the interstellar extinction curve. They fall in the near-ultraviolet to the near-infrared range (NIR) (4400–10000 Å). The bands are characterized as diffuse because of the observation that they are broad and shallow in comparison to the well-known narrow interstellar atomic lines. The individual DIBs vary widely in strength and shape, with equivalent width per magnitude of visual extinction ranging from about 2 Å to the detection limit of about 0.006 Å. The full width at half-maximum (FWHM) values for the DIBs range from about 0.4 to 40 Å.

The features around 5780 and 5797 Å were the first DIBs to be recognized as “stationary” lines in the spectra of spectroscopic binaries (Heger 1922). Their interstellar nature was established by Merrill (1934, 1936) and by Beals & Blanchet (1937). The survey of Herbig (1975) reported 39 DIBs. Since that time, the number of DIBs has been extended to more than 220 (Herbig 1988; Herbig & Leka 1991; Jenniskens & Désert 1994; Krelowski, Sneden, & Hiltgen 1995). The most recently discovered DIBs are very weak with typical equivalent width per magnitude of visual extinction of the order of 0.01 Å.

Despite intense efforts, no definitive identification of the carrier(s) of the DIBs has been made. Various candidates have been proposed as possible carriers for the bands, ranging from impurity-doped dust grains to free, neutral and ionized, molecular species of varying sizes and structures (Tielens & Snow 1995) to molecular hydrogen

(Sorokin & Glowina 1995). It is now clear that the DIBs cannot be explained by the early concept of a single carrier owing to the large number of bands detected and the lack of correlation between the bands. It is now thought that (1) the carriers are large carbon-bearing gas-phase molecules in either the neutral and/or ionized forms and that (2) these molecular carriers are part of an extended size distribution of the interstellar dust (Tielens & Snow 1995). Structure within the profiles of a few strong DIBs is now seen in high-resolution observations. This structure is generally interpreted as the signature of the rotational band structure of gas-phase molecules (Sarre et al. 1995; Ehrenfreund and Foing 1996; Jenniskens et al. 1996; Kerr et al. 1998). Quite recently, laboratory experiments on the gas-phase spectroscopy of various C-chains have shown a good match between the positions and relative intensities of bands of C₇⁻ and six DIBs (Tulej et al. 1998). Higher resolution observations are now required to confirm this potential fit, in particular regarding the fit in relative intensities. Nonetheless, this result supports an origin of the DIBs in C-rich molecules.

The problem of the identification of the DIB carriers is further complicated in that many DIBs overlap (Herbig 1975). For example, the prominent λ 5780 DIB (henceforth, the major bands will be labeled by their approximate central wavelengths in Å) overlaps with the very broad (\approx 20 Å) but extremely shallow λ 5778 DIB. Further structure within the general profile of this broad band has been suggested by Herbig (1975) and demonstrated by Krelowski, Schmidt, & Snow (1997). The latter paper also shows that the weak features are of a different origin and thus they are simply blended with the λ 5778 DIB.

The Doppler splitting of the sharp profiles of interstellar atomic lines also affects the DIB profiles. Herbig & Soderblom (1982) have shown that the very narrow λ 6196 DIB has a complex, Doppler-split profile along some lines of sight. It is now clear that the DIBs observed in the spectra of heavily reddened, distant stars are composed of multiple components, with each originating in individual clouds of different radial velocities and different physical properties. In the case of the broader DIBs, the Doppler splitting is not seen directly, but the resultant profiles are much broader than in single-cloud cases (e.g., Westerlund & Krelowski 1988). It should be emphasized that when the clouds along any sight line produce different spectra (as shown by Krelowski & Westerlund 1988 or Krelowski & Walker 1987), the resulting observation is an ill-defined average spectrum of all these clouds and any interpretation of the data becomes very difficult.

Recent observations have demonstrated that all of the well-known DIBs (i.e., the stronger features) are of different origins (Cami et al. 1997; Moutou et al. 1999). However, Krelowski, Schmidt, & Snow (1997) found that the newly discovered, weak, interstellar features may be related to the strong ones. This implies that the spectrum of any potential DIB carrier consists of a single strong band together with several weak features. Note that this requirement is met by the spectra of PAH ions as discussed below.

It is also important to mention that the study of Moutou et al. (1999) modifies the concept of “families” of diffuse bands initially introduced by Krelowski & Walker (1987). This latest survey shows that the DIB “families” are sets of features the carriers of which coexist in the same clouds, i.e., under the same physical conditions. This does not necessar-

ily imply that the bands belonging to one “family” share a common origin.

3. THE OBSERVATIONAL PROGRAM

The survey, described below, is based on three new sets of observational data. Heavily reddened stars have been selected to facilitate the detection of weak spectral features. In many cases, the same object has been observed with more than one instrument to compare data from different sources and to ensure that the weak features traced in the spectra are real and that their intensities can be measured with a reasonable accuracy.

Most of the spectra discussed here have been acquired with two very similar echelle spectrometers, which allow coverage of the wavelength range from ~ 3500 Å to ~ 10100 Å in one exposure with a resolution of 45,000 as described by Musaev (1993). The spectrometers are fed either with the 1 m Zeiss telescope of the Special Astrophysical Observatory (SAO) of the Russian Academy of Sciences or with the 2 m telescope of the observatory on top of the Terskol peak (Northern Caucasus). The spectrometers are equipped with 1242×1152 CCDs (Wright Instruments; pixel size 22.5×22.5 μm) and can acquire spectra of stars as faint as ~ 9 mag.

The echelle spectra were reduced using the DECH code described by Galazutdinov (1992). This program allows flat-field division, bias/background subtraction, one-dimensional spectrum extraction from the two-dimensional images, diffuse light correction, spectrum addition, removal of cosmic-ray features, etc. The DECH code also allows the location of continuum levels, the measurement of line-equivalent widths, positions, and shifts, etc. The spectral range, covered in every exposure, contains strong and well-identified interstellar atomic lines, Ca II, Ca I, Na I, and K I, for rest-wavelength calibrations.

Some of the spectra have been acquired by one of us (J. K.) at the McDonald Observatory in Texas. The total set of collected spectra contains data for ~ 80 objects—OB stars, more or less reddened. All the spectra cover the wavelength range from ~ 5600 to ~ 7000 Å with a resolution of 60,000 and have been acquired with the Sandiford echelle spectrograph installed at the Cassegrain focus of the 2.1 m telescope. The data acquisition and reduction techniques are described in Krelowski & Sneden (1993). The set of the McDonald spectra contains data for many reddened objects as well as for a few objects considered as unreddened standards, which are in fact very slightly reddened and which are also considered in this survey. The set of

McDonald spectra is characterized by an exceptionally high signal-to-noise ratio from 500 to 1000.

Table 1 lists the objects considered in this paper together with their spectral types, luminosity classes, color excesses, and the apparent rotational velocities. Weak interstellar features, observed in spectra of rapidly rotating stars (HD 210839), cannot be of stellar origin. The observed colors have been taken from the SIMBAD database and the intrinsic colors from the paper by Papaj, Krelowski, & Wegner (1993). We have selected heavily reddened stars to enhance the detection of weak interstellar features. We have also selected stars characterized by different strength ratios for the major DIBs $\lambda\lambda 5780$ and 5797 because it has been shown (Krelowski et al. 1995) that the pattern of the weak features varies with the ratio of the strength of the $\lambda\lambda 5780$ and 5797 DIBs.

4. THE LABORATORY PROGRAM

Matrix isolation spectroscopy (MIS) is used to simulate environmental conditions in the laboratory that are close to the conditions known (or expected) in the diffuse interstellar medium. In MIS experiments, the neutral and ionized PAHs are fully isolated at low temperatures (< 5 K) in the low-polarizability neon matrices where the perturbations induced in the spectrum of the trapped molecules/ions are minimum (Salama 1996). Until PAHs can be routinely studied in supersonic jets, MIS remains the best tool available to simulate the conditions of the diffuse ISM.

The experimental apparatus and protocol have been described elsewhere (Salama & Allamandola 1991; Salama et al. 1994) and only a synopsis is given here. Briefly, the experimental apparatus consists of a cryogenic sample chamber that is part of a high-vacuum system and consists of four ports at 90° and two gas injection ports at 45° . The sample holder suspended at the center of the chamber is cooled down to 4.2 K by a liquid He transfer cryostat. The substrate (sapphire) can be positioned to face alternatively the spectroscopy ports, the gas injection ports, an irradiation lamp, or vacuum deposition furnace. The spectral light sources consist of a 160–360 nm output D₂ lamp and a 320–2500 nm output tungsten filament lamp. The light collected at the spectroscopy port of the sample chamber is guided to the entrance slit of a triple-grating monochromator by a fiber optic cable and detected by a CCD array mounted directly on the exit port and interfaced to the computer system. The ionization source is a microwave-powered, flow-discharge hydrogen lamp generating photons of 10.2 eV energy (Ly α line). The PAH sample is

TABLE 1
BASIC STELLAR DATA

HD or BD	Sp	V	$B - V$	$E(B - V)$	$v \times \sin(i)$	Observatory
183143	B7 Ia	6.84	1.27	1.28	60	Terskol, McDonald
186745	B8 Ia	7.00	+0.93	1.00	126	Terskol
187459	B0.5 I	6.40	0.20	0.41	126	SAO
190603	B1.5 Iae	5.64	0.56	0.73	32	SAO
194279	B1.5 Ia	7.01	1.03	1.20	50	Terskol
195592	O9.5 Ia	7.10	0.87	1.11	300	SAO
207198	O9 IIe	5.95	0.31	0.54	76	Terskol
210839	O6 Iab	5.06	+0.23	0.52	285	McDonald
224055	B3 Ia	7.17	0.70	0.83	45	Terskol
BD +40°4220	O7e	9.10	1.67	1.96	>400	Terskol

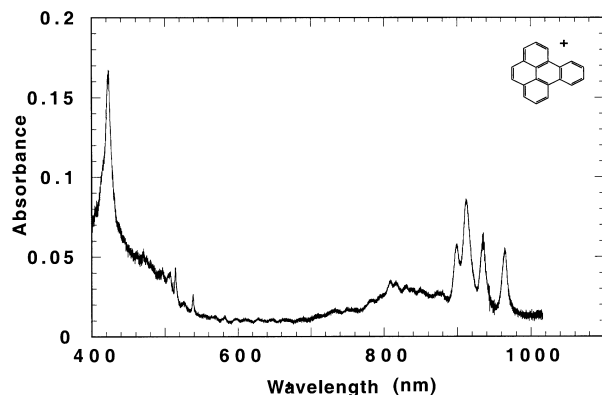


FIG. 1a

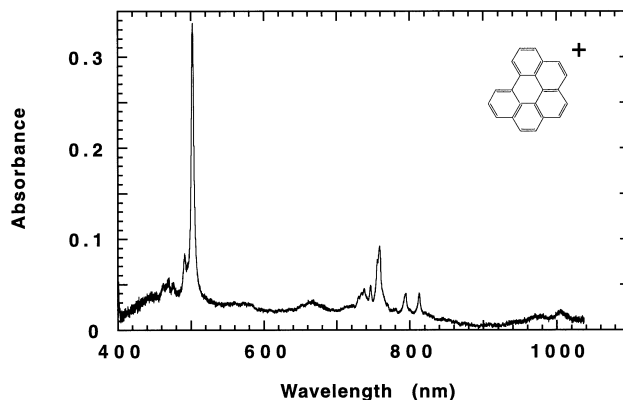


FIG. 1b

FIG. 1.—Laboratory absorption spectra of the (a) benzo(e)pyrene cation ($C_{20}H_{12}^+$) and (b) the benzo(ghi)perylene cation ($C_{22}H_{12}^+$) isolated in Ne matrices at 4.2 K.

simultaneously condensed with the neon gas onto the cold substrate. The frozen matrix is then spectroscopically analyzed. Ions are generated in situ from the stable precursor, via vacuum-ultraviolet (VUV) photoionization.

VUV irradiation of the neutral PAHs isolated in Ne matrices produces *new spectral features* in the UV–NIR range (180–1060 nm). The new features are found to be associated with the PAH cation (PAH^+) formed by direct, one-photon ionization of the neutral precursor. Some representative spectra are shown in Figures 1 and 2 for the PAH cations phenanthrene ($C_{14}H_{10}^+$), benzo(e)pyrene ($C_{20}H_{12}^+$), benzo(ghi)perylene ($C_{22}H_{12}^+$), and pentacene ($C_{22}H_{14}^+$).

The astrophysical implications derived for PAH ions have been discussed in the literature (Salama et al. 1996; Salama 1996) and are recapitulated below:

1. Contrary to their neutral precursors, *ionized PAHs absorb in the visible and NIR and could contribute to the DIBs* (see Figs. 1 and 2). Large PAH ions (≥ 100 rings, i.e., containing more than 250–300 C-atoms) are not expected, however, to contribute significantly to the DIBs because their strongest absorption falls outside the wavelength range in which the DIBs are observed (Salama et al. 1996; Salama 1996).

2. The absorption spectrum of PAH cations is dominated by a single band in the spectral range of interest for comparison with the DIBs (NUV–NIR). The stronger PAH ion transitions measured in Ne are compared in Table 2 with the known DIBs. The fractional shift in energy is well

within the 0.5% shift generally expected between the Ne matrix and gas-phase measurements (Bondybey & Miller 1983; Salama 1996; Romanini et al. 1999).

3. In the case of compact PAHs (such as $C_{16}H_{10}^+$ and $C_{22}H_{12}^+$ shown in Fig. 1), the strongest absorption lies at the high-energy end of the spectrum, and its oscillator strength is of the order of 0.1. In the case of noncompact PAHs (such as $C_{10}H_8^+$, $C_{14}H_{10}^+$, and $C_{22}H_{14}^+$ shown in Fig. 2), the strongest absorption lies at the low-energy end of the spectrum and has an oscillator strength in the range 0.001–0.1.

5. COMPARISON OF ASTRONOMICAL SPECTRA WITH LABORATORY SPECTRA

Figures 3, 4, 5, 6, 7, and 8 show the spectra of heavily reddened stars in the vicinity of the major PAH ion features measured in laboratory experiments. Features were searched for in 100 Å windows around laboratory peak wavelength positions. This criterion for the wavelength width has been chosen to take into account the upper limit to the wavelength shift known to be induced by the solid matrix (Salama 1996). In all the figures, the interstellar spectral features are plotted in the laboratory wavelength scale for the gas-phase lines. Such features are very abundant, especially in the NIR. As shown in § 4 and in Figures 1 and 2, the PAH ion candidates produce one strong band together with several weaker features in the NUV–NIR range.

Table 2 compares the PAH features, measured in the

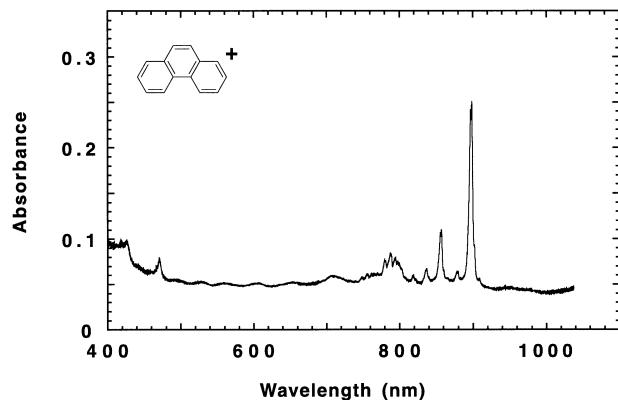


FIG. 2a

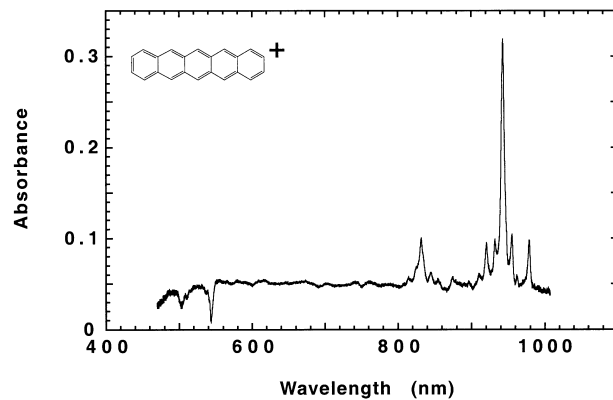


FIG. 2b

FIG. 2.—Laboratory absorption spectra of (a) the phenanthrene cation ($C_{14}H_{10}^+$) and (b) the pentacene cation ($C_{22}H_{14}^+$) isolated in Ne matrices at 4.2 K. Negative features seen around 5000 Å in the spectrum of pentacene are associated with the depletion of the neutral precursor upon ionization.

TABLE 2

COMPARISON OF DIBs WITH THE ABSORPTION BANDS OF PAH CATIONS ISOLATED IN NEON MATRICES

λ PAH ⁺ (Ne matrix data)	HD 207198 Sp = O9 lie $E(B - V) = 0.60$	BD + 40° 4220 Sp = O7e $E(B - V) = 1.96$	HD 195592 Sp = O9.5 Ia $E(B - V) = 1.14$	HD 190603 Sp = B1.5 Iae $E(B - V) = 0.72$	HD 187459 Sp = B0.5 I $E(B - V) = 0.41$
3442 TetracB
4227 B(e)pyrA	Blended with interstellar Ca I (4226.734), 9.5%, 18 mÅ	Interstellar Ca I 4226.73, 5.5%, 4 mÅ	Interstellar Ca I 4226.73, 10 mÅ
4395 PyreneA
4442 1MePyrA	DIB 4428.88, 6.5%, 450 mÅ	DIB 4428.88, 4.5%, 400 mÅ	DIB 4428.88, 3%, 200 mÅ
4456 4MePyrA
4499 COHPyrA	DIB 4501.8, 4%, 140 mÅ	...	DIB 4501.8 blended with stellar lines	DIB 4501.8, 3.5%, 100 mÅ	DIB 4501.8, 2.5%, 63 mÅ
4580 4MePyrB
4590 CoronA
4987 COHPyrB	DIB 4963.96, 4.5%, 31 mÅ DIB 4969.67, 1.2%, 10 mÅ DIB 4984.73, 3%, 13 mÅ	Low S/N (here and above)	DIB 4963.96, 5.5%, 30 mÅ DIB 4969.67, 2%, 30 mÅ DIB 4984.73, 2%, 30 mÅ	DIB 4963.96, 1.5%, 15 mÅ DIB 4969.67, 1.3%, 10 mÅ DIB 4984.73, 1%, 8 mÅ	DIB 4963.96, 2%, 15 mÅ DIB 4984.73, 1.5%, 3 mÅ
5022 b(ghi)perA	...	New feature 5025, 7%, 2 mÅ
5251 PeryIA
6120 NaphIB2 (projected value)*	DIB 6116.65, 2.5%, 19 mÅ	DIB 6116.65, 2%, 9 mÅ	...
6489 NaphIB1*	DIB 6491.88, 4.5%, 22 mÅ	...
6706 NaphIA*	DIB 6699.37, 4%, 23 mÅ DIB 6701.98, 2.2%, 4 mÅ	...	DIB 6699.37, 3%, 15 mÅ	DIB 6699.37, 2%, 19 mÅ	DIB 6699.37, 3%, 20 mÅ DIB 6701.98, 1%, 6.5 mÅ DIB 7224.18, 8%, 125 mÅ
7229 peryIB1	DIB 7224.18, 19%, 200 mÅ	DIB 7224.18, 15%, 200 mÅ	DIB 7224.18, 8%, 125 mÅ
7256 peryIB2	DIB 7257.35, 1%, 15 mÅ DIB 7249.26, 2.8%, 43 mÅ DIB 7276.7, 6%, 33 mÅ	DIB 7224.18, 19%, 200 mÅ DIB 7257.35, 1%, 15 mÅ	DIB 7224.18, 15%, 200 mÅ DIB 7276.7, 2.5%, 20 mÅ
7580 1MePyrB	DIB 7585.63, 1.8%, 30 mÅ (Stellar C m?)	...	DIB 7581.24, 5%, 39 mÅ	DIB 7558.5, 1.5%, 26 mÅ	DIB 7562.24, 3.5%, 30 mÅ
7584 b(ghi)perB	See above	See above	See above	See above	See above
7588 4MePyrC	See above	See above	See above	See above	See above
8321 PentacB	DIB 8283.45, 1.5%, 44 mÅ	New feature DIB 8321, 6.3%, 44 mÅ	DIB 8283.45, 3.5%, 60 mÅ	DIB 8283.45, 3%, 31 mÅ	...
8508 PhenantB*
8648 TetracA	DIB 8621.23, 4.5%, 290 mÅ	DIB 8621.23, 16.6%, 600 mÅ	DIB 8621.23, 7%, 440 mÅ	DIB 8621.23, 7%, 447 mÅ	DIB 8621.23, 6.5%, 650 mÅ
8839 1.2benzantha
8919 PhenantA*
9124 B(e)pyrB
9310 MePhenA
9433 PentacA
9470 CoronB
	...	DIB 9577, 10%, 380 mÅ DIB 9632, 11%, 280 mÅ	DIB 9577, 9%, 300 mÅ DIB 9632, 7.5%, 215 mÅ	DIB 9577, 5%, 200 mÅ DIB 9632 blended with Mg II, 7%, 180 mÅ	...

NOTE—Tetrac: Tetracene, C₁₈H₁₂⁺; B(e)pyr: Benzo(e)pyrene, C₂₀H₁₂⁺; Pyrene: Pyrene, C₁₆H₁₀⁺; 1MePyr: 1-Methylpyrene, CH₃C₁₆H₉⁺; 4MePyr: 4-Methylpyrene, CH₃C₁₆H₉⁺; COHPyr: 1-Pyrenealdehyde, COHC₁₆H₉⁺; Coron: Coronene, C₂₄H₁₂⁺; b(ghi)per: Benzo(ghi)perylene, C₂₂H₁₂⁺; Peryl: Perylene, C₂₀H₁₂⁺; Naphth: Naphthalene, C₁₀H₈⁺; Pentac: Pentacene, C₂₂H₁₄⁺; Phenant: Phenanthrene, C₁₄H₁₀⁺; 1.2benzantha: 1,2-benzanthracene, C₁₈H₁₂⁺; MePhen: Methylphenanthrene, CH₃C₁₄H₉⁺; A = Strongest absorption band in the NUV-NIR range, B = second strongest band, and so forth; *Gas-phase data from CRDS measurements (Romanini et al. 1999) and TOF experiments (Bréchnignac & Pino 1999).

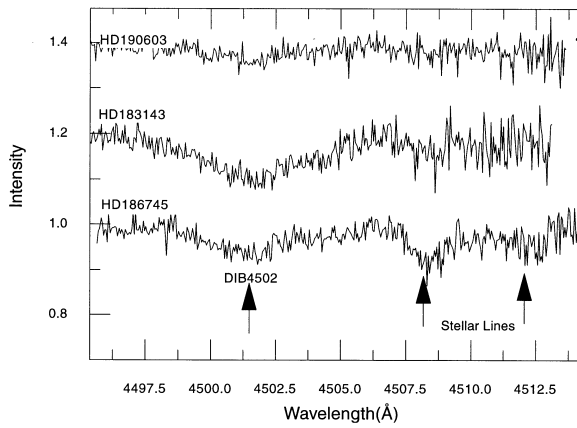


FIG. 3.—Spectral range around the carbohydroxyppyrene ion $[(\text{COH})\text{C}_{16}\text{H}_9^+]$ feature near 4499 Å (laboratory position from MIS experiments). Note the presence of the strong $\lambda 4502$ DIB in its close vicinity.

laboratory, with their possible astronomical counterparts. Here, the window for comparison has been chosen so as to cover a fractional shift of 0.5% in energy for the laboratory-measured absorption bands (Salama 1996). This value is a conservative estimate based on the very limited gas-phase data set that is available for comparison. The shift in band positions induced by a Ne matrix is expected to be small. For example, a gas-phase-to-Ne fractional shift of 0.3%–

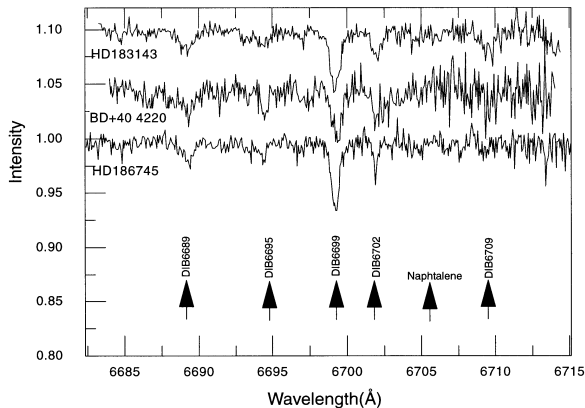


FIG. 4.—Spectral range around the naphthalene ion ($\text{C}_{10}\text{H}_8^+$) feature near 6706 Å (laboratory position from gas-phase experiments of Romanini et al. 1999). Note the presence of several weak and very weak DIBs in its close vicinity.

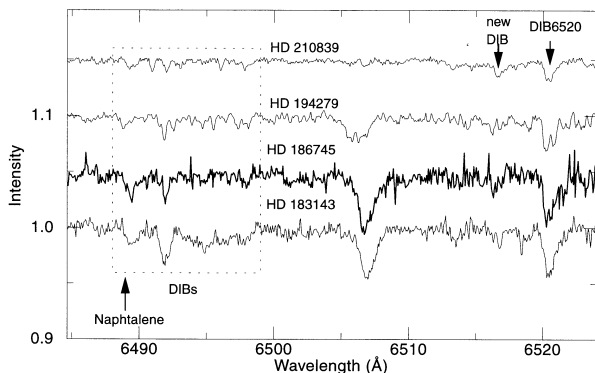


FIG. 5.—Spectral range around the naphthalene ion ($\text{C}_{10}\text{H}_8^+$) feature near 6489 Å (laboratory position from gas-phase experiments of Romanini et al. 1999).

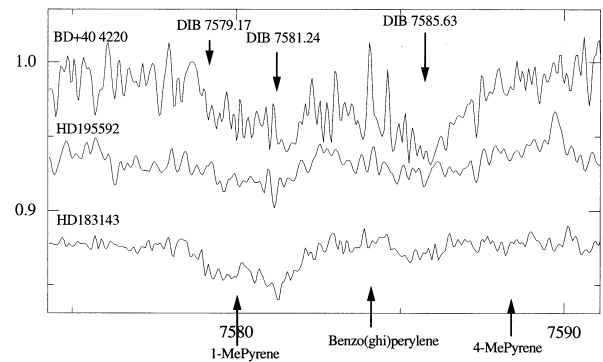


FIG. 6.—Weak interstellar features in the spectra of heavily reddened stars close to the laboratory positions of the 1-methylpyrene ($\text{CH}_3\text{C}_{16}\text{H}_9^+$), benzo(ghi)perylene ($\text{C}_{22}\text{H}_{12}^+$), and 4-methylpyrene ($\text{CH}_3\text{C}_{16}\text{H}_9^+$) ions (laboratory positions from MIS experiments).

0.5% is measured for C_6F_6^+ and its derivatives (Bondybey & Miller 1983), and a value of 0.5% has been derived recently in the case of $\text{C}_{10}\text{H}_8^+$ (Romanini et al. 1999).

6. DISCUSSION

DIBs can be classified roughly as strong (band equivalent widths $W_\lambda \geq 1.0$ Å), moderately strong ($1.0 \text{ Å} \geq W_\lambda \geq 0.1$ Å), and weak ($W_\lambda \leq 0.1$ Å) (Salama et al. 1996). There are only three strong DIBs and fewer than 50 moderately

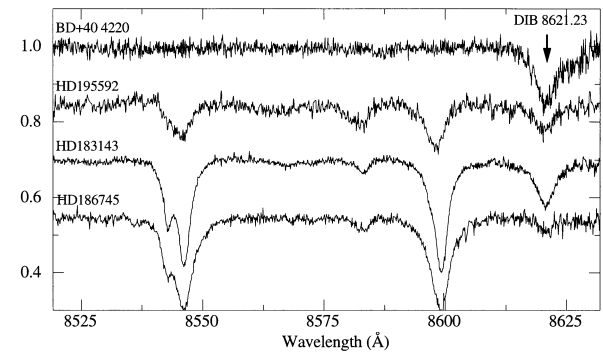


FIG. 7.—Interstellar features in the $\lambda 8525$ – 8625 spectra of heavily reddened stars. Note the presence of the strong $\lambda 8621$ DIB in the close vicinity of the tetracene ion ($\text{C}_{18}\text{H}_{12}^+$) absorption (laboratory position from MIS experiments).

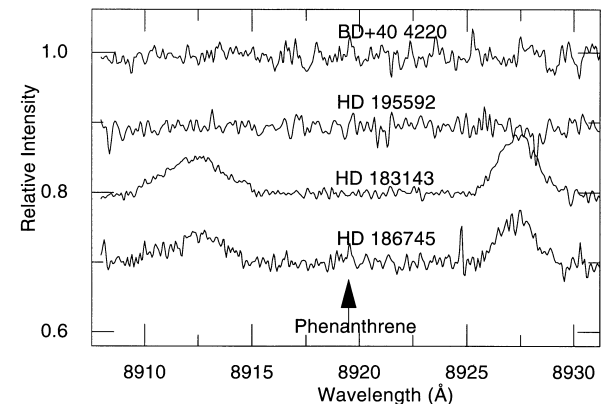


FIG. 8.—Spectral range around the 8919 Å feature of the phenanthrene ion ($\text{C}_{14}\text{H}_{10}^+$). Note the absence of any DIB in its close vicinity (laboratory position from gas-phase experiments of Bréchnignac & Pino 1999).

strong DIBs tabulated in Herbig (1995) toward the star HD 183143. All the rest of the DIBs (i.e., the vast majority) range from weak to very weak (less than 0.01 Å equivalent widths). The recent, high-quality spectra of reddened stars makes it possible to detect hundreds of weak interstellar features reliably. All the weak features exhibit the same characteristics as the well-known stronger DIBs (Ehrenfreund & Foing 1996; Jenniskens et al. 1996; Kerr et al. 1998) and are also most likely of molecular origin. These features are observed in practically all environments, including the very diffuse clouds (Galazutdinov et al. 1998). This indicates that the (molecular) carriers of the weak DIBs must be resistant against the UV-photon background. Although the increased number of observed features provides more clues for the identification of the band carriers, unambiguous assignments are now more complex. Another difficulty arises in that many of the newly observed weak interstellar features fall in the NIR spectral range. This range is also populated with numerous telluric lines, mostly caused by water vapor, which often mask the presence of potential interstellar bands (Galazutdinov et al. 1999). Only in the cases of a very dry atmosphere can the removal of telluric lines be complete.

As illustrated in Figures 1 and 2, the spectrum of a PAH cation in the NUV–NIR spectral range is characterized by a single strong feature and several related weak bands (i.e., weaker by, at least, an order of magnitude). The weaker bands associated with a specific PAH ion are expected to be observed only when the strongest PAH feature is associated with one of the strong, or moderately strong, well-known DIBs. Inversely, if the strongest feature of a PAH ion corresponds to one of the weak DIBs observed in our spectra (i.e., the features observed at the level of detection—see Figs. 3–7), there is, obviously, no possibility of detecting the weaker PAH band relatives, which would be no deeper than 0.001 of the continuum. In other words, there are two scenarios that can be met while attempting to identify specific DIBs with specific PAH ions. First, one has a situation where many absorption bands of a single PAH ion correlate with a combination of strong and weak DIBs. This is the most rewarding situation where a decisive and unambiguous spectral identification can be made based on the comparison of the wavelength positions, energy intervals and relative intensities of numerous bands. Second, one has a situation where the strongest absorption band of a PAH ion correlates with a weak DIB. This in itself does not represent a spectral fit. The assignment gains credibility, however, if a significant number of PAH ions (10 or more) are found to be correlated with weak DIBs. On examining the laboratory (MIS) spectra of PAH ions against these two criteria, it becomes possible to identify a number of PAH ions that could be potential DIB carriers. Of course, because of the small neon-matrix-to-gas-phase shift, the selected PAH ions must then be studied in the gas phase in jet expansions to provide the test for a decisive comparison in wavelengths and band profiles with the astronomical spectra.

Table 2 shows the comparison between the laboratory data for 14 PAH ions and the astronomical bands measured in the spectra of five of the reddened objects listed in Table 1. The window for comparison has been chosen so as to encompass a possible fractional shift of 0.5% in energy for the laboratory MIS absorption bands as compared to the gas phase. This window encompasses, thus, any likely

expected shift induced by the solid neon matrix (see the discussion above). Following this criterion and despite the fact that the weak DIB features are quite abundant in the NIR, it is found that, with the exception of the 7580 Å band of the 1-methylpyrene ion, each specific laboratory band is correlated to no more than three DIBs in most cases (i.e., no more than three DIBs are found in any “error box” centered on the laboratory band position). Table 2 also indicates that about one-third of the elements in the laboratory database (five PAH ions of 14) exhibit a potential correlation with DIBs. Four other PAH cations have their strongest transitions in the range 8800–9400 Å, which is heavily obscured by telluric water vapor bands. Moreover, out of the 24 DIBs found to fall in the wavelength windows, seven can be described as strong to moderately strong while the rest of the bands range from weak to very weak. This comparison leads to the following conclusions.

First, among the five PAH ions that show a clear positive correlation with DIBs, three PAHs—1-methylpyrene, carbohydroxypyrene, and tetracene—correlate with strong to moderately strong DIBs. The other two PAHs, benzo(ghi)perylene and naphthalene, are correlated with very weak DIBs.

Second, among the nine PAH ions that are not detected, five (namely, coronene, perylene, phenanthrene, pyrene, and its derivative 4-methylpyrene) can be ruled out and are not expected to contribute significantly to the DIBs because their strongest absorption is not detected in the astronomical spectra. This conclusion is definitely unambiguous in the case of the phenanthrene ion ($C_{14}H_{10}^+$) since its spectrum has been measured recently in the gas phase (Bréchnignac & Pino 1999), thereby allowing for a direct comparison with the astronomical observations (Fig. 8). The strongest transition of the cold gas phase $C_{14}H_{10}^+$ is reported at 891.9 nm (Bréchnignac & Pino 1999). A careful search for a feature centered at this wavelength in our observational spectra of heavily reddened stars has been negative. This is clearly indicated in Figure 8 where a spectral range of ± 10 Å around the 891.9 nm feature has been chosen to account for any potential residual small van der Waals (vdW) shift induced by the experimental approach (in this technique, the spectrum of the phenanthrene cation is derived from the photofragmentation spectrum of optically selected phenanthrene⁺-argon van der Waals complex cations formed in a molecular beam. The derived spectrum is then corrected for the small vdW redshift [Bréchnignac & Pino 1999]). Note that a previous search for the coronene and ovalene ions in the spectra of five reddened stars (including BD +40°4220) also led to very low upper limits (Ehrenfreund et al. 1995). The case of the four other PAH ions (namely, benzo(e)pyrene, methylphenanthrene, benzanthracene, and pentacene) is less clear. This is because their strongest transition is either blended with an interstellar band (the strongest transition of benzo(e)pyrene is blended with the interstellar Ca I $\lambda 4227$ band [Table 2]) or falls in a region heavily obscured by telluric lines (as in the case of 1-methylphenanthrene, benzanthracene, and pentacene [Fig. 2]). We note, however, that a DIB is observed near the position of the second strongest band of the pentacene ion. We discuss, below, each case of positive correlation.

6.1. 1-methylpyrene⁺

The absorption spectrum of the photolysis product of 1-methylpyrene [$(CH_3)C_{16}H_9$] is dominated by a band at

4442 Å, which falls close to the strong $\lambda 4429$ DIB (0.3% fractional shift). This band has been assigned tentatively to the methylene-pyrene cation. The other very strong band seen in the laboratory spectrum has been shown to belong to a different photolysis product of methylpyrene (Léger, d'Hendecourt, & Défourneau 1995). The weaker 7580 Å band can be correlated to more than one weak DIB in the range 7558–7585 Å, although it is difficult to measure an accurate band ratio from the weak astronomical features (see Table 2 and Fig. 6).

6.2. Carbohydroxypyrene⁺

The absorption spectrum of the photolysis products of carbohydroxypyrene [(COH)C₁₆H₉) is dominated by a band at 4499 Å, which falls close to the moderately strong $\lambda 4502$ DIB shown in Figure 3 (0.07% fractional shift). By analogy with the case of methylpyrene, this band is tentatively assigned to the cation (COH)C₁₆H₉⁺. The other strong band seen in the laboratory spectrum belongs to a different photolysis product of carbohydroxypyrene. The weaker band around 8980 Å falls in the region obscured by telluric lines (Table 2).

6.3. Tetracene⁺

The absorption spectrum of the tetracene ion (C₁₈H₁₂⁺) is dominated by a band at 8648 Å, which falls close to the very strong $\lambda 8621$ DIB shown in Figure 7 (0.3% fractional shift). This correlation is only tentative because the spectrum shows, in this case, strong band splitting induced by the matrix (Table 2). Moreover, the other moderately strong band of the tetracene ion, which falls at 8373 Å, has not been detected yet in the astronomical spectra.

6.4. Naphthalene⁺

The case of the naphthalene ion (C₁₀H₈⁺) has been discussed in detail in a recent paper presenting the first gas-phase spectrum of a PAH ion isolated in an expansion jet (Romanini et al. 1999). One can now directly compare the laboratory spectra to the astronomical spectra. From this preliminary study, it appears that the two strongest bands of C₁₀H₈⁺ fall at 6706 and 6489 Å and may be associated with the very weak $\lambda \lambda 6699$ and 6492 DIBs (see Figs. 4 and 5). The relative intensity of the two bands was found to be the same (~1.8) in the laboratory and in the astronomical observations available at that time (Jenniskens & Désert 1994). However, our recent astronomical survey indicates that the relative intensity of these two bands is variable (from 1.2 to 5.2), making it unlikely that these two bands are of the same origin. This discrepancy between the two astronomical surveys dramatically illustrates the difficulty of accurately measuring the equivalent widths of weak DIBs, as was noted previously (Salama 1996). Moreover, it is likely that the $\lambda 6492$ DIB is blended with the Fe II $\lambda 6491.7$ stellar line in the spectra of HD 183143 and HD 21389 reported by Jenniskens & Désert (1994). The two DIBs also have similar FWHM (0.6 and 0.8 Å, respectively), which are about 20 times narrower than those associated with the naphthalene ion bands (14 and 18 Å, respectively). Moreover, when applying the fractional shift of 0.5% in energy measured between the gas phase (6706 and 6489 Å) and the

neon matrix (6741 and 6520 Å) values to the other strong vibronic band of C₁₀H₈⁺, found at 6151 Å in the Ne matrix, a projected position of 6116 Å is found for this third band in the gas phase. This value is very close to the weak $\lambda 6117$ DIB, which has a width of 0.5 Å. If, alternatively, the strongest of C₁₀H₈⁺ band at 6706 Å is correlated with the very weak $\lambda 6702$ DIB (see Fig. 4), the other vibronic bands of C₁₀H₈⁺ are not detectable. In conclusion, the case of C₁₀H₈⁺ is weak but not yet settled and awaits further laboratory experiments in the gas phase (see Table 2).

6.5. Benzo(ghi)perylene⁺

Finally, in the case of the benzo(ghi)perylene ion, the spectrum is clearly dominated by a band at 5022 Å, which falls close to the very weak $\lambda 5022.4$ DIB (0.01% fractional shift). This makes it impossible to detect the much weaker benzo(ghi)perylene band at 7585 Å (see Table 2 and Fig. 1).

In conclusion, we reiterate that the direct comparison of the MIS spectra of PAH ions with the spectra of selected reddened stars cannot yield to a decisive, unambiguous, identification of DIB carriers. This is because (1) the spectra measured in the laboratory are subject to band position shifts induced by the solid matrix and (2) the stellar spectra contain so many interstellar features that only a precise experimental determination of the wavelengths of molecular features *together* with their gas-phase profile can allow a definitive identification. A comparison between the MIS laboratory data and the astronomical observations is useful, however, when the matrix-to-gas-phase shift is taken into account. The MIS data provide, then, an essential guide for the selection of PAH ions to be spectroscopically studied in a jet expansion (i.e., under conditions that mimic the conditions reigning in the interstellar medium) much more challenging experimentally. The MIS data indicate that a substantial number of PAH ions are promising candidates for the DIB carriers. Out of a laboratory set of only 14 PAH ions that sample compact and noncompact PAHs, hydrogenated PAHs, and PAHs with a heteroatom, five exhibit a positive correlation with DIBs, four cannot be settled, and five can be disregarded as potential DIB carriers. The jet experiments just now being developed will provide the much needed data to definitively assess the validity of the PAH proposal with regard to the DIBs. More astronomical surveys of DIB objects are also needed, especially in the wavelength ranges that have not been observed frequently as yet. The spectrograph used in this project is particularly adapted to this task and will be used to collect an extensive set of high-quality spectra of reddened stars.

This work has been supported by the II US–Poland Maria Skłodowska–Curie Joint Fund under the grant MEN/NSF-94-196. G. A. G. acknowledges the support of the Nicolaus Copernicus University in Toruń. G. A. G. and F. A. M. acknowledge the financial support of the Russian Foundation of Basic Research (Grant 98-02-16544). The laboratory research covered in this review has been supported by grants from NASA (Office of Space Science, Astrophysics program) to F. S.

REFERENCES

- Allamandola, L. J., Tielens, A. G. G. M., & Barker, J. R. 1989, *ApJS*, 71, 733
- Beals, C. S., & Blanchet, G. H. 1937, *PASP*, 49, 224
- Bondybey, V. E., & Miller, T. A. 1983, in *Molecular Ions: Spectroscopy, Structure and Chemistry*, ed. T. A. Miller & V. E. Bondybey (Amsterdam: North-Holland), 138
- Bréchnignac, Ph., & Pino, Th. 1999, *A&A*, 343, 49
- Cami, J., Sonnentrucker, P., Ehrenfreund, P., & Foing, B. H. 1997, *A&A*, 326, 822
- Crawford, I. A. 1989, *MNRAS*, 241, 575
- Crawford, M. K., Tielens, A. G. G. M., & Allamandola, L. J. 1985, *ApJ*, 293, L45
- Ehrenfreund, P., d'Hendecourt, L., Verstraete, L., Léger, A., Schmidt, W., & Defourneau, D. 1992, *A&A*, 259, 257
- Ehrenfreund, P., & Foing, B. H. 1996, *A&A*, 307, L25
- Ehrenfreund, P., Foing, B. H., d'Hendecourt, L., Jenniskens, P., & Désert, F. X. 1995, *A&A*, 299, 213
- Galazutdinov, G. A. 1992, *Preprints Spets. Astrof. Obs.*, No. 92
- Galazutdinov, G. A., Krelowski, J., Moutou, C. & Musaev, F. A. 1998, *MNRAS*, 295, 437
- Galazutdinov, G. A., Krelowski, J., Musaev, F. A., Ehrenfreund, P., & Foing, B. H. 1999, *MNRAS*, submitted
- Heger, M. L. 1922, *Lick Obs. Bull.*, 10, 146
- Herbig, G. H. 1975, *ApJ*, 196, 129
- . 1988, *ApJ*, 331, 999
- . 1995, *ARA&A*, 33, 19
- Herbig, G. H., & Leka, K. D. 1991, *ApJ*, 382, 193
- Herbig, G. H., & Soderblom, D. R. 1982, *ApJ*, 252, 610
- Jenniskens, P., & Désert, X. 1994, *A&AS*, 160, 39
- Jenniskens, P., Porceddu, I., Benvenuti, P., & Désert, X. 1996, *A&AS*, 313, 649
- Krelowski, J., & Papaj, P. 1993, *PASP*, 105, 1121
- Krelowski, J., Schmidt, M., & Snow, T. P. 1997, *PASP*, 109, 1135
- Krelowski, J., & Sneden, C. 1993, *PASP*, 105, 1141
- Krelowski, J., Sneden, C., & Hiltgen, D. 1995, *Planet. Space Sci.*, 43, 1195
- Krelowski, J., Snow, T. P., Seab, C. G., & Papaj, J. 1992, *MNRAS*, 258, 693
- Krelowski, J., & Walker, G. A. H. 1987, *ApJ*, 312, 860
- Krelowski, J., & Westerlund, B. E. 1988, *A&A*, 190, 339
- Kerr, T. H., Hibbins, R. E., Fossey, S. J., Miles, J. R., & Sarre, P. J. 1998, *ApJ*, 495, 941
- Léger, A., & d'Hendecourt, L. B. 1985, *A&A*, 146, 81
- Léger, A., d'Hendecourt, L., & Défourneau, D. 1995, *A&A*, 293, 53
- Mathis, J. S. 1990, *ARA&A*, 28, 37
- Mattila, K., et al. 1996, *A&A*, 315, L353
- Merrill, P. W. 1934, *PASP*, 46, 206
- . 1936, *PASP*, 48, 179
- Morton, D. C. 1975, *ApJ*, 197, 85
- Moutou, C., Krelowski, J., d'Hendecourt, L., & Jamroszczak, J. 1999, *A&A*, in press
- Musaev, F. A. 1993, *Pisma AZh*, 19, 776
- Onaka, T., et al. 1996, *PASJ*, 48, L59
- Papaj, J., Krelowski, J., & Wegner, W. 1993, *A&A*, 273, 575
- Puget, J. L., & Léger, A. 1989, *ARA&A*, 27, 161
- Romanini, D., Biennier, L., Salama, F., Katchanov, A., Allamandola, L. J., & Stoeckel, F. 1999, *Chem. Phys. Lett.*, 303, 165
- Salama, F. 1996, in *Low Temperature Molecular Spectroscopy*, ed. R. Fausto (NATO ASI Ser. 483; Dordrecht: Kluwer), 169
- Salama, F., & Allamandola, L. J. 1991, *J. Chem. Phys.*, 94, 6964
- . 1992a, *ApJ*, 395, 301
- . 1992b, *Nature*, 358, 42
- . 1993, *J. Chem. Soc. Faraday Trans.*, 89, 2277
- Salama, F., Bakes, E. L. O., Allamandola, L. J., & Tielens, A. G. G. M. 1996, *ApJ*, 458, 621
- Salama, F., Joblin, C., & Allamandola, L. J. 1994, *J. Chem. Phys.*, 101, 10252
- . 1995, *Planet. Space Sci.*, 43, 1165
- . 1999, in preparation
- Sarre, P., Miles, J. R., Kerr, T. H., Hibbins, R. E., Fossey, S. J., & Somerville, W. B. 1995, *MNRAS*, 277, L41
- Snow, T. P. 1992, *Australian J. Phys.*, 45, 543
- Sorokin, P. P., & Glowina, J. H. 1995, *Chem. Phys. Letters*, 234, 1
- Tielens, A. G. G. M., & Snow, T. P., eds. 1995, *IAU Colloq. 137, The Diffuse Interstellar Bands* (Dordrecht: Kluwer)
- Tulej, M., Kirkwood, D. A., Pachkov, M., & Maier, J. 1998, *ApJ*, 506, L69
- Van der Zwet, G. P., & Allamandola, L. J. 1985, *A&A*, 146, 76
- Westerlund, B. E., & Krelowski, J. 1988, *A&A*, 203, 134
- Whittet, D. C. B. 1996, in *ASP Conf. Ser. 97, Polarimetry of the Interstellar Medium*, ed. W. G. Roberge and D. C. B. Whittet (San Francisco: ASP), 125